Viscous flow and heat transfer through two coaxial porous cylinders

Jacques Hona[1,*], Elkana Pemha[1] and Elisabeth Ngo Nyobe[2]
[1]Applied Mechanics Laboratory, Faculty of Science,
University of Yaoundé I, P.O. Box 7389 Yaoundé,
Cameroon, E-mail address: elkanaderbeau@yahoo.fr
[2]Department of Mathematics and Physical Science,
National Advance School of Engineering,
University of Yaoundé I, P.O. Box 8390 Yaoundé,
Cameroon, E-mail address: nyobe_eli@yahoo.fr

ABSTRACT
In this paper, a flow of a high viscous fluid with temperature-dependent viscosity through a porous industrial conduct is investigated by means of similarity transformation technique. The problem is modeled using mass, momentum and energy conservations. The variation of viscosity as function of temperature couples the vorticity equation to the energy equation. The numerical procedure for solving the differential equations of the problem is detailed. For low values of the main control parameters, the analytical solution of the problem is yielded. It appears from the numerical results of the problem that the variations of temperature are stopped in a large area around the middle of the flow domain. The maxima of thermal gradients are situated at the walls due to suction. The dominance of flow reversal agrees with the behavior of the normal pressure gradient inside the annular conduct.

Keywords: Nonlinear two-point boundary-value problem, Detailed numerical integration, Similarity solutions, Variable viscosity, Viscous flows, Porous annular conducts

1. INTRODUCTION

Several investigations of fluid flows are performed by solving the Navier-Stokes equations. [1–5]. In the studies of flows through channels with thermal effects, the channels usually have a rectangular configuration or a cylindrical configuration as in the investigation of plane Poiseuille flows [2] or the study of heat transfer in rectangular ducts or circular tubes [3]. Other works exist where the effects of temperature on fluid flows are intensively examined [6–8]. When the channel admits porosity or wall motion, the problem is relative to a Berman flow because the pioneer work of Berman [9] on a laminar flow in a porous rectangular channel without thermal effects has inspired many other studies [10–12]. In particular those which extended the Berman analysis for establishing the existence of symmetric and asymmetric solutions under certain critical values of the Reynolds numbers [13–18]. Many works followed [19–23] discussing the existence of solutions as function of control parameters. In most cases where the flows are two-dimensional, a similarity transformation is applied to produce a single nonlinear ordinary differential equation.

*Corresponding Author: E-mail: honajacques@yahoo.fr Tel.: +237 91 36 44 75

Flows through porous channels or tubes are on the basis of several applications. These applications include petroleum industry, filtration, paper manufacturing, membrane separation processes, transpiration cooling, biological transport processes, solar energy collectors, and also the control of boundary layer separation with suction or injection.

In the present study, the viscous flow through the porous annulus is governed by the Navier-Stokes equations relative to velocity components and the energy equation satisfied by temperature. Equal fluxes of fluid are established at both uniformly porous walls of the annulus. The behavior of viscosity depends on the temperature difference between the walls. There exist similarity solutions of the type introduced by Berman, but modified by the existence of a variable high viscosity. To describe the dependence of viscosity on temperature, many possible laws exist in the literature. The usual ones are linear, [24, 2] algebraic [7, 24] or exponential behaviors [2, 5, 6]. The variation of the dynamic viscosity while other properties of the fluid remain constant couples the Navier-Stokes equations to the energy equation. If the temperature difference between the walls of the annulus is not high enough to produce significant changes in the dynamic viscosity, the Navier-Stokes equations and the energy equation are in partial coupling [25]. In fact, this partial coupling is due to the correlation in terms of the stream function and thermal gradients through the energy equation. However, if the viscosity varies with temperature as in the present work, the equations describing the flow are fully coupled. At this stage, it is relevant to signal that the novelty in this study is the investigation of the effects of viscosity gradients on the high viscous flow occurring through a porous annular industrial conduct. Although this viscosity varies with temperature, it remains high enough, so that inertial terms of the Navier-Stokes equations are neglected.

The annular pipe has walls at a and $a + 2h$. Hence, the width of the annulus is $2h$ as shown in Fig. 1. The mass withdrawal phenomenon occurs with suction speed V at both uniformly porous walls of cylinders. The annulus consists of a cold inner cylinder at temperature T_0 and a hot outer cylinder at temperature T_1, such that $T_1 > T_0$. The value of viscosity at temperature T_0 is μ_0 taken as the reference value with respect to the behavior of the variable dynamic viscosity. Other physical properties of the fluid which remain constant are the specific mass ρ and the thermal conductivity κ.

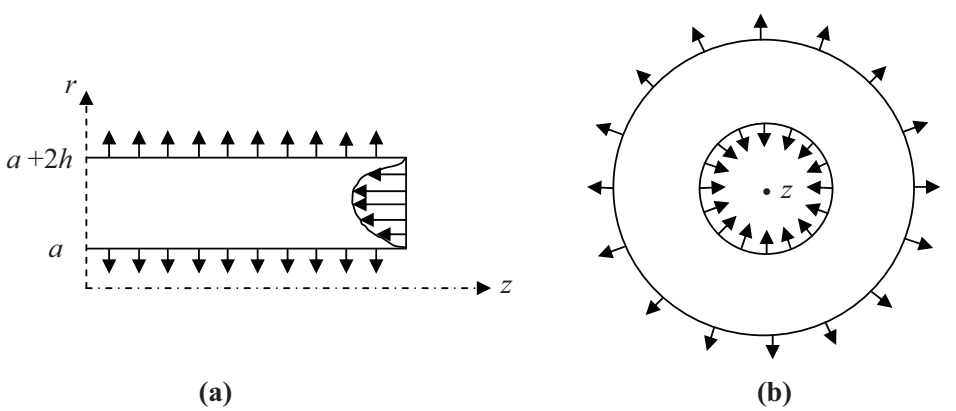

Figure 1: Geometry of the annulus: (a) Half-flow region with a typical axial velocity profile and suction occurring at walls, (b) Section of the annulus with suction at $r = a$ and $r = a + 2h$

The strategy consists to introduce the stream function in the governing equations of the problem. A similarity transformation is then applied to obtain two coupled nonlinear ordinary differential equations satisfied by the stream function and temperature in nondimensional formulation. Some analyses are performed after finding the solutions of the problem in order to extend the numerical results to physical significant settings.

2. DYNAMIC MODEL OF THE FLOW

To start, it is important to note that the creeping flow occurs when the fluid is considered highly viscous so that inertial terms of the momentum equation are neglected compared to viscous terms [26, 27].

In the problem under study, dimensionless variables are taken in units of length (h), velocity (V), temperature ($\Delta T = T_1 - T_0$), pressure (ρV^2), and viscosity (μ_0), then the Reynolds number $R = \rho Vh/\mu_0$ and the Péclet number $P = \rho Vh/\kappa$ are derived. In all that follows, the variables are nondimensional.

A cylindrical polar coordinate system (r, ϕ, z) is adopted such that r represents the radial coordinate, ϕ is the angular coordinate, and z denotes the axial coordinate. The z-axis is the symmetry axis of the annular tube. Since the flow is assumed to be axisymmetric, the velocity field has components as (v, 0, w), where v is the radial velocity and w the axial one. The variables for temperature and pressure are T and p, respectively. The annulus is supposed to be horizontal with the length in the z-direction tending to infinity in order to neglect the influences at the ends, while the width $2h$ holds constant.

The assumption that the flow is axisymmetric enables to define the stream function φ with respect to the two non-vanished velocity components v and w by a well known relation in order to satisfy mass conservation. The introduction of the stream function is accompanied by a new temperature function Θ which takes into account the difference of temperatures between the walls. Functions φ and Θ are given as follows:

$$v = -\frac{1}{r}\frac{\partial \varphi}{\partial z}, \quad w = \frac{1}{r}\frac{\partial \varphi}{\partial r}$$

$$T(r,z) = \Theta(r) + \frac{T_0}{T_1 - T_0} \tag{1}$$

Considering mass, momentum and energy conservations, the stream function φ satisfies the vorticity transport equation while function Θ describes the energy equation by neglecting dissipation effect which could occur inside the annular tube. These governing equations are:

$$\mu D^4\varphi + \left(2\frac{\partial}{\partial r}\left(D^2\varphi\right) - \frac{D^2\varphi}{r}\right)\frac{\partial \mu}{\partial r} + \left(\frac{\partial^2\varphi}{\partial r^2} - \frac{\partial^2\varphi}{\partial z^2} - \frac{1}{r}\frac{\partial \varphi}{\partial r}\right)\frac{\partial^2 \mu}{\partial r^2} = 0 \tag{2}$$

$$\frac{1}{r}\frac{\partial \varphi}{\partial z}\frac{\partial \Theta}{\partial r} + \frac{1}{P}\left(\frac{\partial^2\Theta}{\partial r^2} + \frac{1}{r}\frac{\partial \Theta}{\partial r}\right) = 0 \tag{3}$$

where $D^2\varphi = (\partial^2\varphi/\partial z^2) + r(\partial/\partial r)((1/r)(\partial\varphi/\partial r))$. The boundary conditions are given by:

$$\frac{1}{r}\frac{\partial \varphi}{\partial z} = 1, \quad \frac{1}{r}\frac{\partial \varphi}{\partial r} = 0, \quad \text{and} \quad \Theta = 0, \quad r = \frac{a}{h}$$

$$\frac{1}{r}\frac{\partial \varphi}{\partial z} = -1, \quad \frac{1}{r}\frac{\partial \varphi}{\partial r} = 0, \quad \text{and} \quad \Theta = 1, \quad r = \frac{a+2h}{h} \tag{4}$$

3. METHOD OF SOLUTION

This stage is about the use of a similarity transformation technique suitable to the geometrical configuration of the annulus. Indeed, we introduce new variables in terms of the nondimensional stream function, temperature, and viscosity as follows:

$$\begin{gathered}\varphi(r,z) = (\delta^{-1}-1)\, z f(x)\\ \Theta(r) = (1-\delta)\,\theta(x)\\ \mu(\theta) = 1-\lambda\,(1-\delta)\theta\\ x = \frac{1}{2}\delta r^2 - \frac{1}{2}\delta^{-1}(1+\delta^2)\\ \lambda = -(\partial\mu/\partial\theta)/(1-\delta)\\ \delta = h/(a+h)\end{gathered} \tag{5}$$

where x is a dimensionless variable which varies between -1 and $+1$, for $r = a/h$ and $r = (a+2h)/h$, respectively. The geometric parameter δ is defined on the basis of the radii of the inner cylinder and the outer one, and the valid interval for this parameter is $0 < \delta < 1$ for the annular viscous flow. The temperature-dependent viscosity undergoes a linear law through the annulus and its behavior gives rise to the existence of a nondimensional parameter λ, called the sensitivity of viscosity to thermal variations, which depends on the fluid properties and on the temperature difference between the walls. Applying the transformations of eqns (5), the differential equations of the problem and the boundary conditions become

$$\begin{gathered}\big(1-\lambda(1-\delta)\theta\big)\Big((1+\delta^2+2\delta x)f^{(4)} + 4\delta f^{(3)}\Big) - 2\lambda(1-\delta)(1+\delta^2+2\delta x)\theta^{(1)} f^{(3)}\\ +\lambda(1-\delta)\big(P(1-\delta)f - 2\delta\big)\theta^{(1)} f^{(2)} = 0\\ (1+\delta^2+2\delta x)\theta^{(2)} + 2\delta\theta^{(1)} + P(1-\delta) f\theta^{(1)} = 0\\ f(-1) = 1, \quad f(1) = -(1+\delta)(1-\delta)^{-1}\\ f^{(1)}(-1) = 0, \quad f^{(1)}(1) = 0\\ \theta(-1) = 0, \quad \theta(1) = (1-\delta)^{-1}\end{gathered} \tag{6}$$

where $f^{(i)} = d^i f/dx^i$ and $\theta^{(i)} = d^i\theta/dx^i$. It follows that, by means of the similarity technique, the axisymmetric viscous flow through the porous annular tube is reduced to a two-point boundary-value problem with three boundary conditions at each wall. This problem admits a geometric parameter δ which describes the nonlinear ordinary differential equations and the boundary conditions. In the case of uniform viscosity (when λ tends to zero) and when the Péclet number P tends to zero, the vorticity equation and the energy equation are linear differential equations providing analytical solutions. We find

$$\begin{gathered}f(x) = a_0 + a_1 x + a_2 x^2 + a_3(1+\delta^2+2\delta x)\ln(1+\delta^2+2\delta x)\\ \theta(x) = a_4 + a_5 \ln(1+\delta^2+2\delta x)\end{gathered} \tag{7}$$

where a_0, a_1, a_2, a_3, a_4 and a_5 are the constants of integration given by

$$a_0 = 1 - \frac{(1-\delta)^{-1}(2\delta + \delta\ln((1+\delta)/(1-\delta)) + 2(1+\delta^2)\ln(1-\delta))}{2\delta - (1+\delta^2)\ln((1+\delta)/(1-\delta))}$$

$$a_1 = -\frac{2\delta(1-\delta)^{-1}\left(1+\ln(1-\delta^2)\right)}{2\delta-(1+\delta^2)\ln((1+\delta)/(1-\delta))}, \quad a_2 = -\frac{\delta(1-\delta)^{-1}\ln((1+\delta)/(1-\delta))}{2\delta-(1+\delta^2)\ln((1+\delta)/(1-\delta))}$$

$$a_3 = \frac{(1-\delta)^{-1}}{2\delta-(1+\delta^2)\ln((1+\delta)/(1-\delta))}, \quad a_4 = -\frac{(1-\delta)^{-1}\ln(1-\delta)}{\ln((1+\delta)/(1-\delta))}, \quad a_5 = \frac{(1-\delta)^{-1}}{2\ln((1+\delta)/(1-\delta))}$$

In addition, negative values of λ are related to some gases where viscosity increases as function of temperature. Positive values of λ correspond to most liquids whose viscosity decreases with temperature. When λ and P are not close to zero, the differential equations are nonlinear and require a numerical integration to be solved.

By considering the expressions of eqns (1), we derive the components of the velocity field as

$$v = -(1-\delta)(1+\delta^2+2\delta x)^{-1/2} f(x)$$
$$w = (1-\delta) z f^{(1)}(x) \tag{8}$$

Considering the momentum conservation, the next characteristics to determine are the normal pressure gradient and the axial pressure gradient per unit length which are given respectively by the following formulas:

$$\frac{\partial p}{\partial x} = \frac{(1-\delta)}{R}\left(2\lambda(1-\delta)\theta^{(1)} f^{(1)} - \mu f^{(2)} - 2\delta\lambda(1-\delta)(1+\delta^2+2\delta x)^{-1}\theta^{(1)} f\right)$$

$$\frac{1}{z}\frac{\partial p}{\partial z} = \frac{\mu(1-\delta)}{R}\left(2\delta f^{(2)} + (1+\delta^2+2\delta x) f^{(3)}\right) - \frac{\lambda(1-\delta)^2}{R}(1+\delta^2+2\delta x)\theta^{(1)} f^{(2)} = \text{constant} \tag{9}$$

For a given Reynolds number in accordance with the creeping flow, the axial pressure gradient per unit length is constant in the annular tube, since it is equivalent to the integral of the left hand side of the similarity vorticity equation. The axial pressure gradient per unit length is usually constant in space when the flow occurs with variable viscosity as in a previous study [8].

4. NUMERICAL STRATEGY

To start, we transform the boundary value problem (6) into an initial value one at point $x = -1$. Since only three conditions are provided at point $x = -1$, such that $f(-1) = 1$, $f^{(1)}(-1) = 0$, $\theta(-1) = 0$, then, to well formulate the initial value problem, it is mandatory to add three additional arbitrary conditions ($f^{(2)}(-1) = \alpha_1, f^{(3)}(-1) = \alpha_2, \theta^{(1)}(-1) = \alpha_3$). To solve the initial value problem applying the fourth-order Runge-Kutta algorithm, we rewrite the ordinary eqns (6) as a system of six first-order coupled differential equations by setting: $f_1 = f$, $f_2 = f^{(1)}$, $f_3 = f^{(2)}$, $f_4 = f^{(3)}$, $\theta_1 = \theta$, $\theta_2 = \theta^{(1)}$. Hence, the six first-order coupled differential equations and the initial conditions are presented as follows:

$$\begin{aligned}
\theta_1^{(1)} &= \theta_2 \\
f_1^{(1)} &= f_2 \\
f_2^{(1)} &= f_3 \\
f_3^{(1)} &= f_4 \\
\theta_2^{(1)} &= -(2\delta\theta_2 + P(1-\delta) f_1\theta_2)/(1+\delta^2+2\delta x) \\
f_4^{(1)} &= 2\lambda(1-\delta) f_4\theta_2/(1-\lambda(1-\delta)\theta_1)
\end{aligned} \tag{10}$$

$$-\left(4\delta f_4 + \lambda(1-\delta)\left(P(1-\delta)f_1 - 2\delta\right)\theta_2 f_3 / (1-\lambda(1-\delta)\theta_1)\right) / (1+\delta^2+2\delta x)$$

$$f_1(-1)=1,\ f_2(-1)=0,\quad f_3(-1)=\alpha_1,\quad f_4(-1)=\alpha_2,\quad \theta_1(-1)=0,\quad \theta_2(-1)=\alpha_3$$

For any arbitrary triplet (α_1, α_2, α_3), and by means of the fourth-order Runge-Kutta algorithm, the values of functions f, θ and those of their derivatives are calculated. Thus, the three boundary conditions at the endpoint $x = 1$, $f_1(1,\alpha_1, \alpha_2, \alpha_3) = f(1, \alpha_1, \alpha_2, \alpha_3)$; $f_2(1, \alpha_1, \alpha_2, \alpha_3) = f^{(1)}(1\ \alpha_1, \alpha_2, \alpha_3)$; $\theta_1(1,\alpha_1, \alpha_2, \alpha_3) = \theta(1, \alpha_1, \alpha_2, \alpha_3)$ are also calculated. More precisely, this means that the solution of the problem depends on α_1, α_2 and α_3.

The best triplet (α_1*, α_2*, α_3*) is the one for which the boundary conditions of the problem at the endpoint $x = 1$, $f(1, \alpha_1, \alpha_2, \alpha_3) = -(1+\delta)(1-\delta)^{-1}$, $f^{(1)}(1,\alpha_1, \alpha_2, \alpha_3) = 0$, $\theta(1, \alpha_1, \alpha_2, \alpha_3) = (1-\delta)^{-1}$ are satisfied. This means that the determination of α_1*, α_2* and α_3* is an optimization type problem. In other words, in seeking the required values of the three guesses, we minimize the following function

$$F(\alpha_1,\alpha_2,\alpha_3) = (f(1,\alpha_1,\alpha_2,\alpha_3)+(1+\delta)(1-\delta)^{-1})^2 + (f^{(1)}(1,\alpha_1,\alpha_2,\alpha_3)-0)^2$$
$$+(\theta(1,\alpha_1,\alpha_2,\alpha_3)-(1-\delta)^{-1})^2 \tag{11}$$

For computing the zeros α_1*, α_2*, α_3* of function F, we apply an algorithm based on the Newton's generalized technique which enables to update the initial guesses as follows:

$$\begin{bmatrix}\alpha_1\\ \alpha_2\\ \alpha_3\end{bmatrix}_{n+1} = \begin{bmatrix}\alpha_1\\ \alpha_2\\ \alpha_3\end{bmatrix}_{n} - [J]^{-1}\cdot\begin{bmatrix} f(1,\alpha_1,\alpha_2,\alpha_3)+(1+\delta)(1-\delta)^{-1}\\ f^{(1)}(1,\alpha_1,\alpha_2,\alpha_3)\\ \theta(1,\alpha_1,\alpha_2,\alpha_3)-(1-\delta)^{-1}\end{bmatrix} \tag{12}$$

where n denotes the iteration index and $[J]^{-1}$ is the inverted Jacobian matrix. The Jacobian itself is given by:

$$J = \begin{bmatrix} \frac{\partial F_1}{\partial\alpha_1} & \frac{\partial F_1}{\partial\alpha_2} & \frac{\partial F_1}{\partial\alpha_3}\\ \frac{\partial F_2}{\partial\alpha_1} & \frac{\partial F_2}{\partial\alpha_2} & \frac{\partial F_2}{\partial\alpha_3}\\ \frac{\partial F_3}{\partial\alpha_1} & \frac{\partial F_3}{\partial\alpha_2} & \frac{\partial F_3}{\partial\alpha_3}\end{bmatrix} = \begin{bmatrix} u_1(1) & u_2(1) & u_3(1)\\ u_1^{(1)}(1) & u_2^{(1)}(1) & u_3^{(1)}(1)\\ q_1(1) & q_2(1) & q_3(1)\end{bmatrix} \tag{13}$$

The quantities F_1, F_2 and F_3 are defined as follows:

$$\begin{aligned} F_1 &= f(1,\alpha_1,\alpha_2,\alpha_3)+(1+\delta)(1-\delta)^{-1}\\ F_2 &= f^{(1)}(1,\alpha_1,\alpha_2,\alpha_3)\\ F_3 &= \theta(1,\alpha_1,\alpha_2,\alpha_3)-(1-\delta)^{-1}\end{aligned} \tag{14}$$

The new functions u_j and q_j, j = 1, 2, 3, are derived as :

$$\boldsymbol{u}_j(x,\alpha_1,\alpha_2,\alpha_3) = \frac{\partial f}{\partial\alpha_j},\qquad \boldsymbol{q}_j(x,\alpha_1,\alpha_2,\alpha_3) = \frac{\partial\theta}{\partial\alpha_j} \tag{15}$$

It follows that the components of the Jacobian matrix are the values of functions $\boldsymbol{u}_j$, $\boldsymbol{u}_j^{(1)}$ and $\boldsymbol{q}_j$ at the endpoint $x = 1$. In fact, functions $\boldsymbol{u}_j$ and $\boldsymbol{q}_j$ are solutions of three sets of coupled

differential equations obtained by taking the derivative of the set of eqns (10) with respect to α_j, j =1, 2, 3, knowing that:

$$\frac{\partial f^{(i)}}{\partial \alpha_j} = \frac{\partial}{\partial \alpha_j}\left(\frac{\partial^i f}{\partial x^i}\right) = \frac{\partial^i}{\partial x^i}\left(\frac{\partial f}{\partial \alpha_j}\right) = u_j^{(i)}$$
$$\frac{\partial \theta^{(i)}}{\partial \alpha_j} = \frac{\partial}{\partial \alpha_j}\left(\frac{\partial^i \theta}{\partial x^i}\right) = \frac{\partial^i}{\partial x^i}\left(\frac{\partial \theta}{\partial \alpha_j}\right) = q_j^{(i)} \tag{16}$$

In this work, the solutions of the problem are interpreted in terms of viscosity, velocity components, temperature, thermal gradients and pressure gradient.

5. RESULTS AND DISCUSSION

The fluid should have in all circumstances a positive dynamic viscosity. For this reason, the valid values of the sensitivity of viscosity to thermal variations are such as $\lambda < 1$. The data from the numerical integration reveal that the results are similar with any value of the geometric parameter in its valid interval $0 < \delta < 1$. In this investigation, the calculations are made for $\delta = 0.3$. The flow is fully influenced by the Péclet number and the sensitivity of viscosity to thermal variations, instead of the Reynolds number. This is in accordance with the creeping flows which occur with small or very moderate velocities, this leads to the following interval for the Péclet number $0 < P < 20$. Away from the above precisions about λ, δ and P, our numerical scheme looses its efficiency. On the other hand, the results are all the more accurate as the values of the control parameters are taken in their respective valid intervals.

5.1. VISCOSITY

Important variations of viscosity are only observed in the neighborhood of the hot wall according to Fig. 2(a) because at fixed conductivity, the viscosity is very sensitive to high temperature. This viscosity decreases with the sensitivity of viscosity to thermal variations near the hot wall, but under different values of the parameter λ, it tends to be constant in a large area, from the cold wall to the center of the flow field. For a fixed negative sensitivity of viscosity to thermal variations, the solution branches of viscosity corresponding to different conductivities tend to a same constant curve in the above described area as shown in Fig. 2(b). But with the low values of the Péclet number, the temperature-dependent viscosity tends to undergo the behavior related to that of the analytical solution of temperature found in Section 3 by referring to the dotted curve of Fig. 2(b) plotted for $P = 0.2$. Thus, the curves presented in Fig. 2(b) show that the viscosity decreases with the Péclet number.

When the parameter λ takes a positive fixed value, a large area of inflection appears through the solution branches computed under different values of the Péclet number as presented in Fig. 2(c). In this figure, the viscosity decreases near the both walls but is almost constant in a large area away from the walls in any branch of solution for $P > 0.2$. A very rapid decrease is observed in the neighborhood of the hot wall since the viscosity is revealed very sensitive to high temperature. The temperature-dependent viscosity undergoes different behaviors as function of the Péclet number due to the sign of the sensitivity of viscosity to thermal variations because it diminishes with the Péclet number when the parameter λ is negative according to Fig. 2(b), but it increases with the Péclet number when the parameter λ is positive by referring to Fig. 2(c). The dotted curve of Fig. 2(c) computed for $P = 0.2$ highlights the fact that the inflection disappears with the decrease of the Péclet numbers.

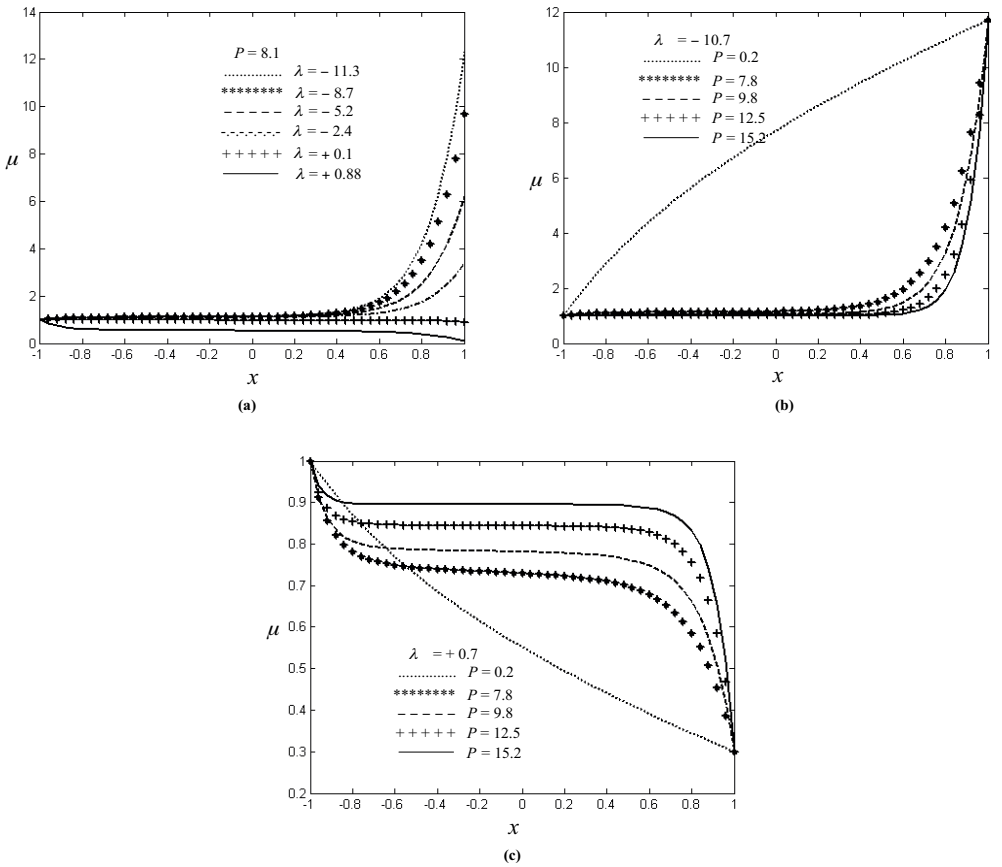

Figure 2: Temperature-dependent viscosity: (a) at fixed conductivity under different values of the sensitivity of viscosity to thermal variations, (b) at fixed negative sensitivity of viscosity to thermal variations under different conductivities (c) at fixed positive sensitivity of viscosity to thermal variations under different conductivities

5.2. AXIAL AND NORMAL VELOCITY PROFILES

Almost all values of the axial velocity per unit length are negative as shown in Fig. 3. This involves the dominance of flow reversal in the annular tube which manifests itself as a parabolic behavior through the axial velocity. Comparing to previous studies where inertial terms are not neglected [15, 21, 25], it follows that the high fluid viscosity in the present work is favorable to flow reversal. However, there are some zones situated at the vicinity of the hot wall where the axial velocity per unit length exceeds it value at walls. This is most noticeable for $\lambda = -11.3$ and $\lambda = -8.7$ at a fixed Péclet number $P = 8.1$ in Fig. 3(a) and for $P = 7.8$, $P = 9.8$ and $P = 12.5$ at a fixed negative sensitivity of viscosity to thermal variations $\lambda = -10.7$ in Fig. 3(b). This noticed scenario of the axial velocity exceeding its value at walls is due to the presence of collision zones in the annulus due to the simultaneous existence of flow reversal and suction which causes the axial velocity to overflow in the neighborhood of the hot wall. Those collision zones have been observed in other studies [28, 29]. For a fixed positive value of the parameter λ the flow is totally reversed under different conductivities according to Fig. 3(c). In this latter figure, the axial velocity profiles tend to the same

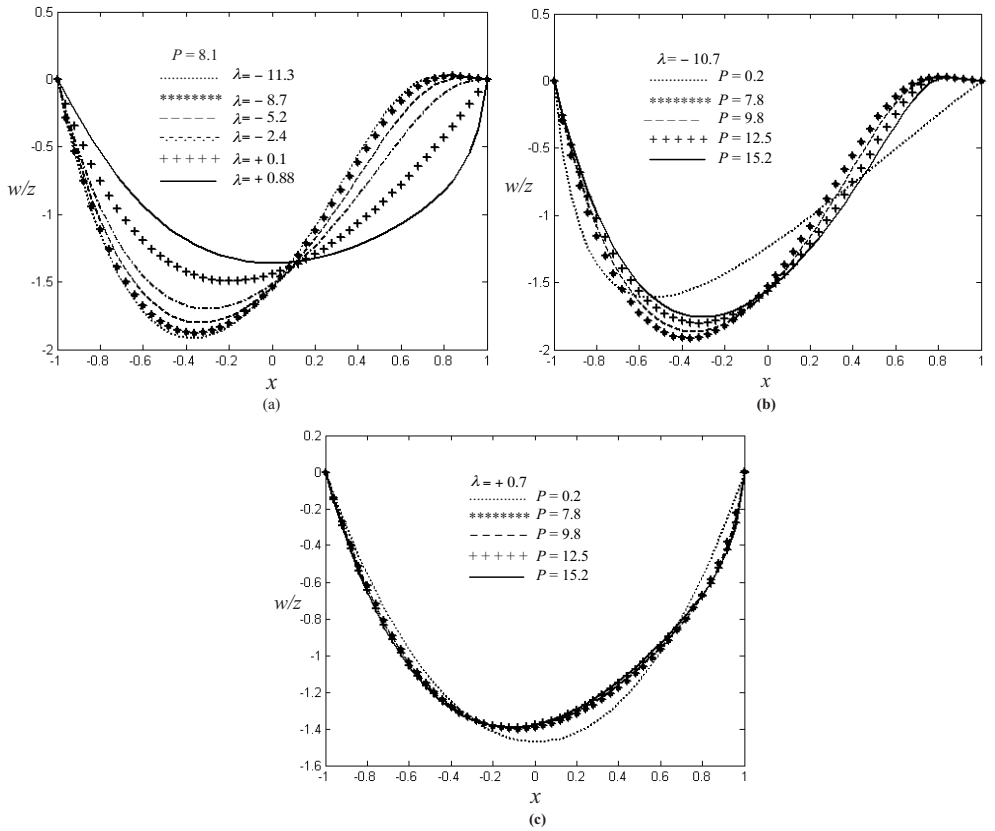

Figure 3: Axial velocity profiles per unit length: (a) at fixed Péclet number for various sensitivities of viscosity to thermal variations, (b) at fixed negative sensitivity of viscosity to thermal variations for various conductivities, (c) at fixed positive sensitivity of viscosity to thermal variations for various conductivities

constant curve because flow reversal is not sensitive to the difference of conductivities at a fixed positive sensitivity of viscosity to thermal variations.

The axial velocity per unit length as plotted in Fig. 3(a) presents two areas of different behaviors inside the annular tube. Indeed, it increases with the parameter λ in the left hand side of the center of the flow region, but decreases in the right hand side. That is because the walls of the annular tube are kept at different temperatures. The same scenario is observed with the Péclet number P at fixed negative sensitivity of viscosity to thermal variations in Fig. 3(b).

The normal velocity overflows near the hot wall as shown in Figs. 4(a) and 4(b) on the same solution branches which present the minimum values of the axial velocity corresponding to the dominance of flow reversal. In fact, it seems that the mass withdrawal phenomenon which occurs at walls is accompanied by flow reversal scenario in order to satisfy mass conservation, such that a fluid particle which leaves the annulus for suction motion is attempted to be replaced with another particle which occupies the empty space thus created. This particular behavior of the flow is envisaged due to the high viscosity of the fluid. The normal velocity as furnished in Fig. 4(a) decreases with the sensitivity of viscosity

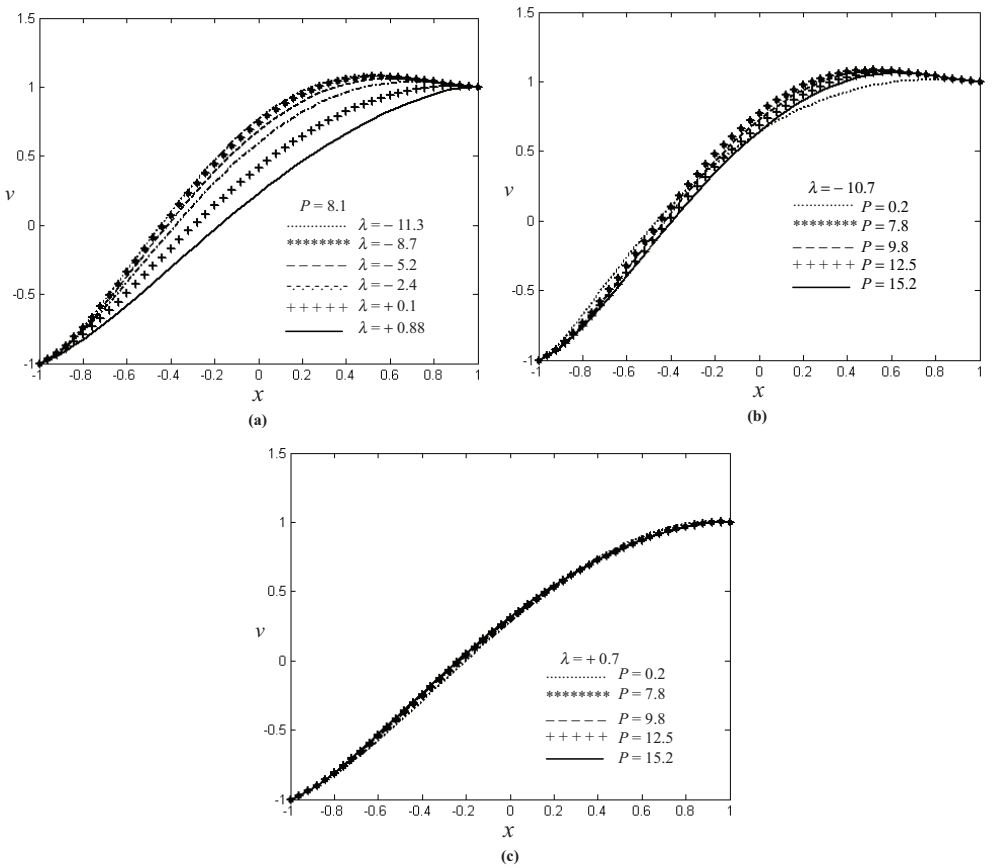

Figure 4: Normal velocity profiles: (a) at fixed Péclet number for various sensitivities of viscosity to thermal variations, (b) at fixed negative sensitivity of viscosity to thermal variations for various conductivities, (c) at fixed positive sensitivity of viscosity to thermal variations for various conductivities

to thermal variations at a fixed Péclet number. Its behavior is similar under different Péclet numbers at a fixed negative parameter λ as illustrated in Fig. 4(b).

The normal velocity profiles under different conductivities at a fixed positive sensitivity of viscosity to thermal variations tend to a same constant curve in Fig. 4(c). This behavior holds because at a fixed positive parameter λ the normal velocity is not very sensitive to the changes happening with respect to the conductivity.

5.3 TEMPERATURE

The temperature distribution at a fixed Péclet number furnished in Fig. 5(a) presents a large area of inflection which disappears with the decrease of the sensitivity of viscosity to thermal variations. This area of inflection is due to the fact that, there is a rapid increase of temperature only at the vicinity of the walls, but not in the rest of the annulus. Thus, Fig. 5(a) shows that the temperature increases with the sensitivity of viscosity to thermal variations, but with the decrease of the parameter λ it tends to zero in a large zone except in the neighborhood of the hot wall. The inflection disappears in Fig. 5(b) at a fixed

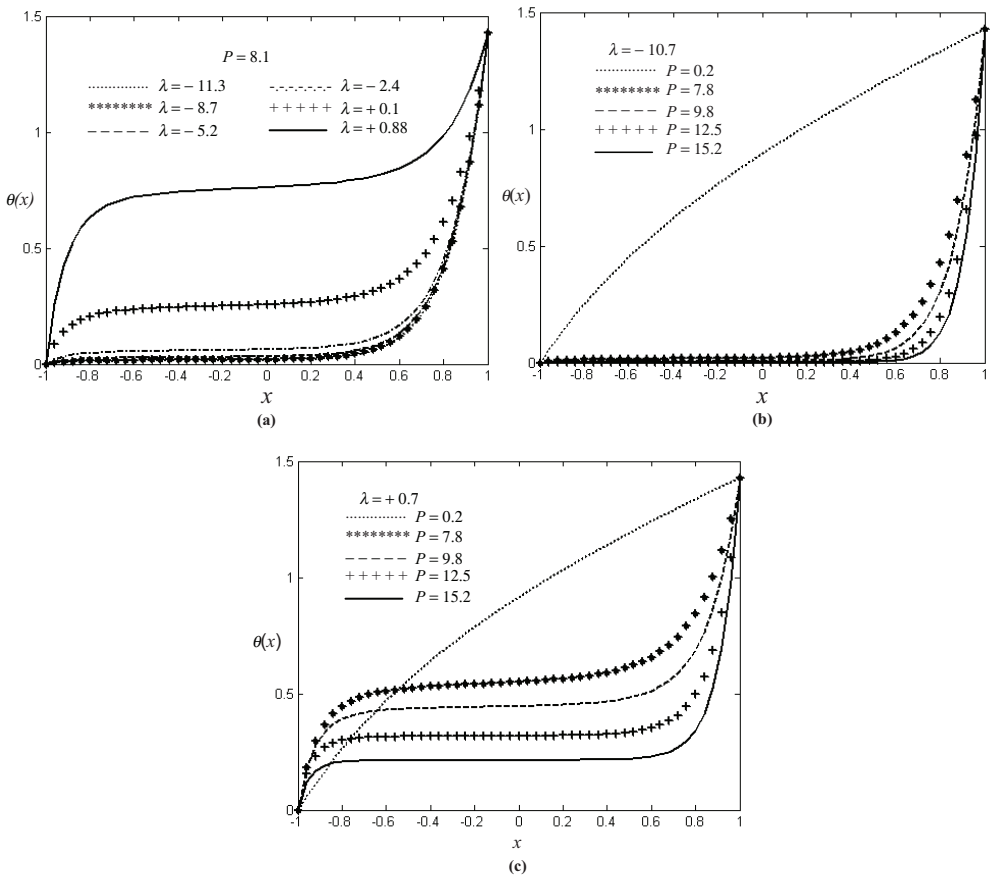

Figure 5: Temperature distribution inside the annulus: (a) at fixed Péclet number for different sensitivities of viscosity to thermal variations, (b) at fixed negative sensitivity of viscosity to thermal variations for different Péclet numbers, (c) at fixed positive sensitivity of viscosity to thermal variations for different Péclet numbers

negative value of the parameter λ under different conductivities. At this level, the rapid growth of temperature is only observed near the hot wall for moderate Péclet numbers. In Fig. 5(b) the temperature decreases with the Péclet number and tends again to zero in a large region as a same constant curve through the annulus except at the vicinity of the hot wall. For the low Péclet number $P = 0.2$, the curve tends to the zero-order analytical solution found in Section 3.

The described inflection appears again in the case of a fixed positive parameter λ for different Péclet numbers as shown in Fig. 5(c). But this inflection disappears with the decrease of the Péclet number. The curves plotted in Figs. 5(b) and 5(c) show that the temperature decreases with the Péclet number. The role of the inflection through the temperature distribution as illustrated in Figs. 5(a) and 5(c) is to cancel the growth of temperature around the middle of the flow region. In Fig. 5, the temperature is always constant around the middle of the flow region in each branch of solution, because in many circumstances, suction is favorable to thermal variations at the vicinity of the walls and prevents the variations of temperature around the center of the flow region.

5.4. THERMAL GRADIENTS

Since the variations of temperature are stopped in a large area around the middle of the flow domain, thermal gradients in that area are canceled, except the case of low Péclet numbers as shown in Fig. 6. These thermal gradients tend to zero and are represented as a same constant curve from the cold wall to the zone around the center of the domain containing the fluid in the case of a fixed negative sensitivity of viscosity to thermal variations by referring to Fig. 6(b). It follows that, when the parameter λ takes negative values, thermal gradients are not very sensitive to the changes happening with respect to different moderate Péclet numbers away from the hot wall. Suction causes rapid variations of thermal gradients near the both walls as shown in Figs. 6(a) and 6(c). Thus, the maxima of thermal gradients are located at the walls. The increase of the parameter λ is favorable to thermal gradients near the cold wall, but is adverse to thermal gradients at the vicinity of the hot wall according to Fig. 6(a). More precisely, a branch of solution with the maximum thermal gradient at the cold wall is the one with the minimum thermal gradient at the hot wall. This highlights the antagonistic behavior between the sensitivity of viscosity to thermal variations and thermal gradients near the walls for the case of fixed conductivity.

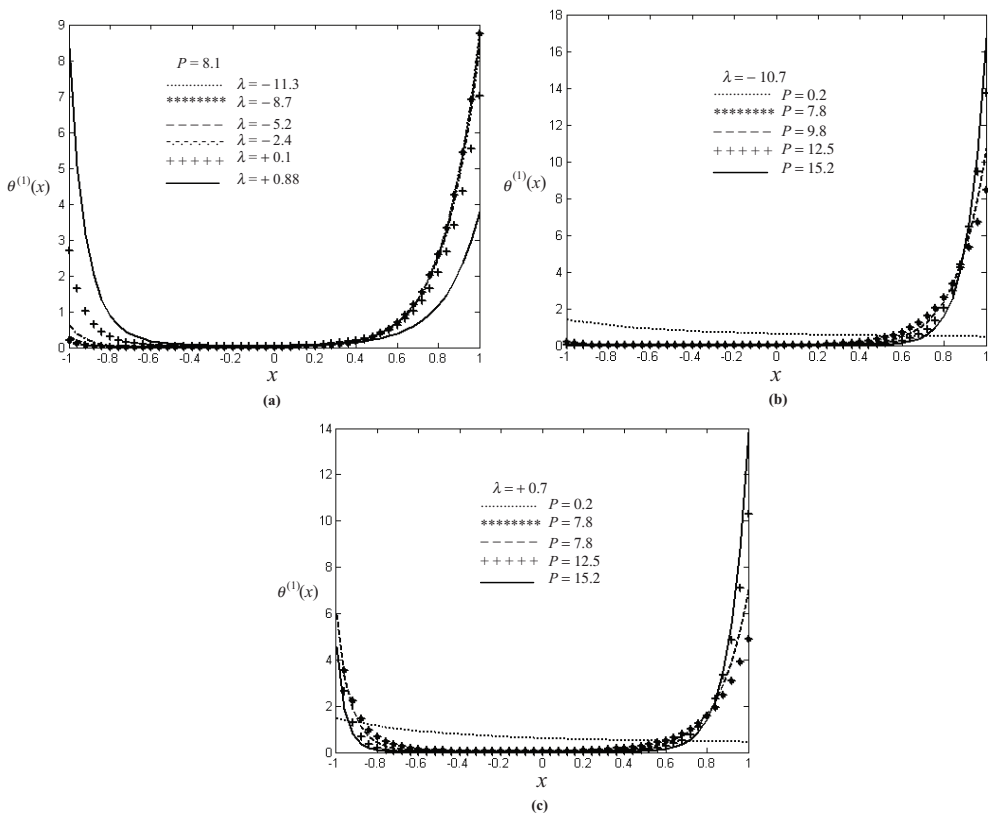

Figure 6: Thermal gradients inside the annulus: (a) at fixed Péclet number for different sensitivities of viscosity to thermal variations, (b) at fixed negative sensitivity of viscosity to thermal variations for different Péclet numbers, (c) at fixed positive sensitivity of viscosity to thermal variations for different Péclet numbers

In light of Fig. 6(a), rapid decreases are observed near the cold wall while rapid increases take place in the neighborhood of the hot wall and the curves are indistinguishable under different values of the parameter λ around the middle of the flow region. That behavior which is due to the inflection occurring in the temperature distribution causes the computed curves of thermal gradients in Fig. 6(a) to present a parabolic structure.

For the case of a fixed negative sensitivity of viscosity to thermal variations, as the effects of different moderate Péclet numbers are only distinguishable near the hot wall as illustrated in Fig. 6(b), one can understand that, thermal gradients increase with the Péclet number near the hot wall. The same behavior is updated in Fig. 6(c) for the case of a fixed positive parameter λ. However, at the cold wall, Fig. 6(c) shows that, those thermal gradients decrease with the Péclet number. In other words, the effects of negative and positive parameter λ on thermal gradients are similar at the hot wall as the Péclet number increases. In all cases, the minima of thermal gradients are located at the center of the flow region while the maxima are situated at the walls.

5.5. PRESSURE GRADIENTS

A fixed value of the Reynolds number is required in order to present the results about pressure gradients. In accordance with the creeping flow, the results are achieved for $R = 1$. The attention is focused on the normal pressure gradient since the axial pressure gradient per unit length is constant at a given Reynolds number.

The normal pressure gradient exhibited in Fig. 7(a) at a fixed conductivity and for various sensitivities of viscosity to thermal variations shows the great changes near the hot wall, because the normal pressure is very sensitive to high temperature. Noticeable changes are also observed with respect to the sign of the parameter λ since different behaviors take place with negative and positive values of the sensitivity of viscosity to thermal variations. Indeed, function $p^{(1)}(x)$ plotted in Fig. 7(a) tends to a same constant curve from the cold wall to the neighborhood of the hot wall for $\lambda = -11.3$, $\lambda = -8.7$, $\lambda = -5.2$ and $\lambda = -2.4$. However, for $\lambda = +0.1$ and $\lambda = +0.88$ the above described behavior disappears such that the branch of solution corresponding to $\lambda = +0.1$ presents a constant line from the cold wall to the hot wall. When $\lambda = +0.88$ the curve presents two concavities which highlight the presence of a large area of inflection.

According to Fig. 7(b), moderate Péclet numbers cancel the normal pressure gradients away from the hot wall at a fixed negative sensitivity of viscosity to thermal variations. Significant variations are only observed in the whole annulus for $P = 0.2$. In other words, away from the hot wall, the normal pressure gradient is not sensitive to the changes happening with moderate Péclet numbers as it tends to zero as a same constant curve under different conductivities.

At a fixed positive sensitivity of viscosity to thermal variations, the normal pressure gradient decreases with the Péclet number as shown in Fig. 7(c). At this stage, the assumption that the inflection tends to occur in Fig. 7(a) for positive parameters λ is confirmed in Fig. 7(c) under various moderate values of the Péclet number. In fact, function $p^{(1)}(x)$ increases rapidly near the two walls, but is constant away from the walls in each branch of solution computed for $P = 7.8$, $P = 9.8$, $P = 12.5$ and $P = 15.2$. On the other hand, in Fig. 7(c), function $p^{(1)}(x)$ is always negative. This behavior agrees with the dominance of the reverse flow described in Fig. 3(c) with the same values of parameters. Hence, the normal pressure gradient is negative in many circumstances due to the dominance of flow reversal on suction through the annulus.

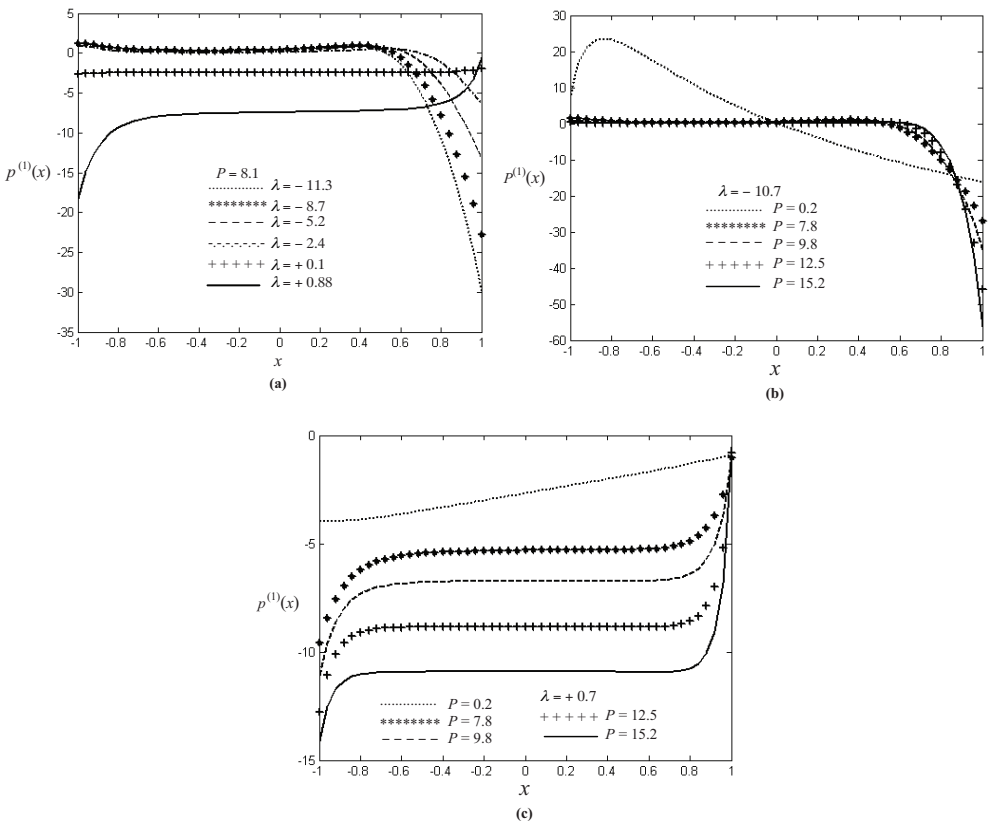

Figure 7: Normal pressure gradients: (a) at fixed conductivity under different values of the sensitivity of viscosity to thermal variations, (b) for a given negative sensitivity of viscosity to thermal variations under different Péclet numbers, (c) for a given positive sensitivity of viscosity to thermal variations under different Péclet numbers

6. CONCLUSION

In seeking the similarity solutions for a viscous flow through a porous annulus, the geometric parameter δ is introduced considering the radii of the two coaxial cylinders. The sensitivity of viscosity to thermal variations λ and the Péclet number P govern the analysis of numerical results.

The zero-order analytical solution is produced when the sensitivity of viscosity to thermal variations and the Péclet number tend to zero. When these parameters are not close to zero, the problem is nonlinear and a numerical integration applying the shooting technique combined with the rapidly converging fourth-order Runge-Kutta algorithm is used to solve the differential equations. The results from the numerical integration enable to confirm that when λ is negative, the temperature-dependent viscosity increases with temperature, but it decreases for positive values of λ. The axial velocity per unit length reveals the dominance of the reverse flow as it presents a parabolic behavior under different values of control parameters. Due to certain values of control parameters, the temperature evolution presents a large area of inflection inside the annulus because suction causes important variations of temperature at the vicinity of the walls while there are not enough variations away from the walls. Thus, the maxima of thermal gradients are located at the walls. The dominance of flow reversal takes place because the normal pressure gradient is in many circumstances negative. The results about the normal pressure gradient agree with those of velocity components.

REFERENCES

[1] Watanabe, T., Numerical Simulation of Oscillating Flow Field Including a Droplet, *The International Journal of Multiphysics*, 2013, 7(1), 19–30.

[2] Schäfer, P. and Herwig, H., Stability of Plane Poiseuille Flow with Temperature Dependent Viscosity, *International Journal of Heat and Mass Transfer*, 1993, 36(9), 2441–2448.

[3] Raithby, G., Laminar Heat Transfer in the Thermal Entrance Region of Circular Tubes and Two-dimensional Rectangular Ducts with Wall Suction and Injection, *International Journal of Heat and Mass Transfer,* 1971, 14(2), 223–243.

[4] Herwig, H. and Schäfer, P., Influence of Variable Properties on the Stability of Two-dimensional Boundary Layers, *Journal of Fluid Mechanics*, 1992, 243, 1–14.

[5] Lin, C.-R. and Chen, C.-K., Effect of Temperature Dependent Viscosity on the Flow and Heat Transfer over an Accelerating Surface, *Journal of Physics D*, 1994, 27(1), 29–36.

[6] Wylie, J. J. and Lister, J. R., The Effect of Temperature Dependent Viscosity on flow in a Cooled Channel with Application to Basaltic Fissure Eruptions, *Journal of Fluid Mechanics*, 1995, 305, 239–261.

[7] Ockendon, H. and Ockendon, J. R., Variable Viscosity Flows in Heated and Cooled Channels, *Journal of Fluid Mechanics*, 1977, 83, 177–190.

[8] Ferro, S. and Gnavi, G., Effect of Temperature-dependent Viscosity in Channels with Porous Walls, *Physics of Fluids*, 2002, 14(2), 839–849.

[9] Berman, A. S., Laminar Flow in Channels with Porous Walls, *Journal of Applied Physics*, 1953, 24(9), 1232–1235.

[10] Terrill, R. M., Laminar Flow in Uniformly Porous Channel, *Aeronautical Quarterly*, 1964, 15(3), 299–310.

[11] Terrill, R. M. and Shrestha G. M., Laminar Flow through Parallel and Uniformly Porous Walls of Different Permeability, *Journal of Applied Mathematics and Physics*, 1965, 16(4), 470–482.

[12] Dinarvand, S., Doosthoseini, A., Doosthoseini, E. and Rashidi, M.M., Comparison of HAM and HPM Methods for Berman's Model of Two-dimensional Viscous Flow in Porous Channel with Wall Suction or Injection, *Advances in Theoretical and Applied Mechanics*, 2008, 1(7), 337–347.

[13] Sellars, J. R., Laminar Flow in Channels with Porous Walls at High Suction Reynolds Number, *Journal of Applied Physics*, 1955, 26(4), 489–490.

[14] Proudman, I., An Example of Steady Laminar Flow at Large Reynolds Number, *Journal of Fluid Mechanics*, 1960, 9, 593–602.

[15] Robinson, W. A., The Existence of Multiple Solutions for the Laminar Flow in a Uniformly Porous Channel with Suction at Both Walls, *Journal of Engineering Mathematics*, 1976, 10(1), 23–40.

[16] Zaturska, M. B., Drazin, P. G. and Banks, W. H. H., On the Flow of a Viscous Fluid Driven along a Channel by Suction at Porous Walls, *Fluid Dynamics Research*, 1988, 4(3), 151–178.

[17] Cox, S.M., Two-dimensional Flow of a Viscous Fluid in a Channel with Porous Walls, *Journal of Fluid Mechanics*, 1991, 27, 1–33.

[18] Banks, W. H. H. and Zaturska, M. B., On Flow through a Porous Annular Pipe, *Physics of Fluids A*, 1992, 4(6), 1131–1141.

[19] Majdalani, J. and Flandro, G. A., The Oscillatory Pipe Flow with Arbitrary Wall Injection, *Proceedings of the Royal Society of London A*, 2002, 458(2023), 1621–1651.

[20] Majdalani, J. and Zhou, C., Moderate-to-large Injection and Suction Driven Channel Flows with Expanding and Contracting Walls, , 2003, 83(3), 181–196.

[21] Dauenhauer, C.E. and Majdalani, J., Exact Self-similarity Solution of the Navier-Stokes Equations for a Porous Channel with Orthogonally Moving Walls, Physics of Fluids, 2003, 15(6), 1485–1495.

[22] Li, B., Zheng, L., Zhang, X. and Ma, L., The Multiple Solutions of Laminar Flow in a Uniformly Porous Channel with Suction/Injection, *Advance Studies in Theoretical Physics*, 2008, 2(10), 473–478.

[23] Lu, C., On the Asymptotic Solution of Laminar Channel Flow with Large Suction, *SIAM Journal on Mathematical Analysis*', 1997, 28(5), 1113–1134.

[24] Stewartson, K., *The Theory of Boundary Layers in Compressible Fluids*, Oxford University Press, Oxford, 1964.

[25] Hona, J., Ngo Nyobe, E. and Pemha, E., Dynamic Behavior of a Steady Flow in an Annular Tube with Porous Walls at Different Temperatures, *International Journal of Bifurcation and Chaos*, 2009, 19(9), 2939–2951.

[26] Brown, H. R., Rayleigh-Taylor Instability in a Finite Thickness Layer of a Viscous Fluid, *Physics of Fluids A*, 1989, 1(5), 895–896.

[27] Davis, A.M.J. and Frenkel, A.L., Cylindrical Liquid Bridges Squeezed between Parallel Plates: Exact Stokes Flow Solutions and Hydrodynamic Forces, *Physics of Fluids A*, 1992, 4(6), 1105–1109.

[28] Brady, J.F., Flow Development in a Porous Channel or Tube, *Physics of Fluids*, 1984, 27(5), 1061–1067.

[29] Brady, J. F. and Acrivos, A. Steady Flow in a Channel or Tube with an Accelerating Surface Velocity. An Exact Solution to the Navier-Stokes Equations with Reverse Flow, *Journal of Fluid Mechanics*, 1981, 112, 127–150.